مجلة كلية التربية الاساسية
كلية التربية الاساسية – الجامعة المستنصرية
Journal of the College of Basic Education Vol.30 (NO. 125) 2024, pp. 1-16

Effect of Annealing Temperature on Structural And Optical Properties of SnO_2 Thin Films

Hiba R. Shakir (1)
1Department of Optometry, Technical Medical Institute-Al-Mansur, Middle Technical University, Iraq
hiba.rashid@mtu.edu.iq

Salah Kaduri Haza'a (2)
Al-Karkh University of Science, College of Science, Department of Medical Physics, Iraq
salah.hazaa@kus.du.iq

Abstract:

SnO_2 thin films were prepared by DC magnetron sputtering technique on glass substrates at 200 ℃ temperature. Both an X-ray diffractometer and a UV/VIS spectrophotometer were used to examine how the annealing temperature affected the structural and optical characteristics of the films. X-ray diffraction patterns indicated that the SnO_2 films showed a polycrystalline tetragonal structure. The optical properties and dispersion parameters of the films have been studied over a wavelength (300-900) nm. A high optical energy-gap of 3.72 eV was achieved at temperature 400 ℃. Many optical parameters such as refractive index, dielectric constant, ratio of carrier concentration to the effective mass, single oscillator energy, dispersive energy, moments of the optical spectrum, the average operator strength, single operator wavelength, optical resistivity, thermal emission, and optical conductivity parameters were determined and examined in relation to the annealing temperature.

Keywords: SnO_2, Optical properties, Dispersion parameters, DC. magnetron sputtering, Annealing, Structure.

Introduction:

Tin Oxide SnO_2films has a high energy band gap (3.7 eV), strong optical transparency, and low electrical resistance within the electromagnetic spectrum's visible range. and low electrical resistance are widely used for many applications, particularly as transparent electromagnetic shielding materials, an electrode material in light emitting diodes, solar cells, etc [1].

The properties of SnO_2 films such as its, optical properties, structure and dispersion parameters … etc can be varied by preparation method. SnO_2 has been created using several techniques such as chemical vapor deposition [2], electron beam evaporation [3], sol gel coating [4], spray pyrolysis [5], magnetron sputtering [6] etc. However, among these methods, magnetron sputtering is significant due to a number of benefits, including the ability to build films at low deposition temperatures, control over the deposition rate, excellent purity, and homogeneity of the coating over wide substrate surfaces [7]. Furthermore, numerous studies are presented with an emphasis on how various factors (such as substrate type and temperature, deposition rate, oxygen partial pressure, and annealing temperature) affect the optical, electrical, and structural characteristics of SnO_2 thin films.

The annealing procedure is one of the most significant variables that may influence SnO_2 thin-film characteristics. Mohamed and Hadia[8] examined The influence of post-thermal annealing on SnO2 optical properties produced using the electron beam evaporation method. In this work, the investigation focused on studying how the annealing temperature impacts the optical dispersion and structural characteristics the DC magnetron sputtering method of growing SnO_2 thin films on glass substrates.

Many optical parameters such as carrier concentration to effective mass ratio, dielectric constant, and refractive index, single oscillator energy, dispersive energy, moments of the optical spectrum, the single oscillator's wavelength and average oscillator strength, optical conductivity, the values of optical resistivity and thermal emissivity were computed. and analysed with relation to the temperature of annealing.

Experimental

The SnO_2 were deposited by means of DC magnetron sputtering operating at a temperature of 200 ℃ On glass substrates. An oil-diffusion pump operating at $2x10^{-6}$ was employed to empty the vacuum chamber, while an Edwards 306 pumping system was employed to remove the vacuum. The experiment lasted 30 minutes and was carried out in a pressurized chamber with 95% argon and 5% oxygen. Here were the factors to consider: 40W direct current where there has to be sufficient energy, electron mobility, and a force that permits the gases to come into close contact with one another, 370 gauss magnetic field, and 30 mm gap between cathode and substrate holder. The glass base was treated with tin oxide that was expelled from targets. The target materials are 60 mm diameter, 2 mm thick SnO_2 powder plates. Thickness film measured by Figure (1) displays an image obtained using scanning electron microscopy (SEM). which was 800±10 nm. Film was post-deposition annealed at (300, 400 and 500) ℃ for 1 hour. The SnO_2 films' structural characteristics were examined utilizing a 1.5406 Å wavelength Cu (Kα) X-ray diffractometer (XRD). At normal incidence, a double-beam spectrophotometer was used to record the spectrum of optical absorbance and transmittance of each film in the (300-900 nm) spectrum range.

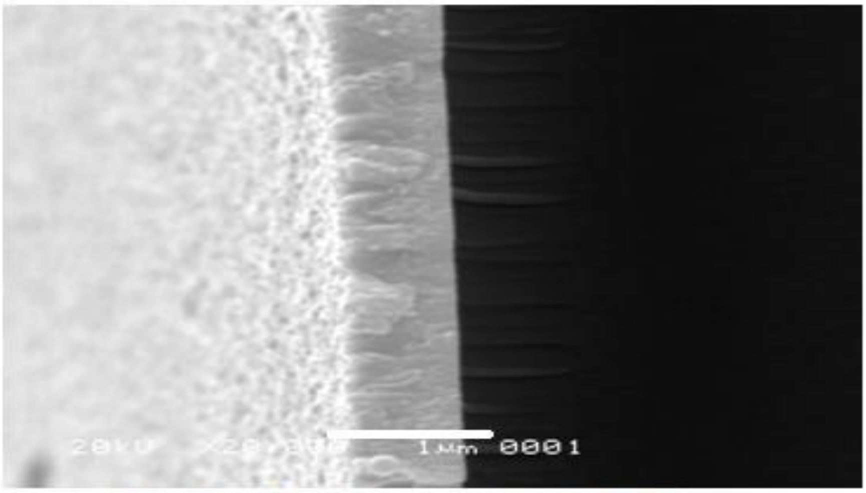

Fig.1. SEM picture of SnO_2 thickness

Results and discussion

Figure (2) displays the SnO2 films X-ray diffraction patterns for samples that were heated to 200 ℃ as-deposited and for samples that were annealed in air for 1 hour at 300, 400, and 500 ℃. According to Table 1, all of the films include one phase of SnO_2 and have a polycrystalline tetragonal structure. One possible reason for the emergence of strain relief at the crystal grains might be for the small changes in diffraction angles and interplanar of the crystal planes change slightly before and after annealing [9]. Crystalline size D values prior to and following annealing, which are around 14.4 nm and 26.3 nm, respectively, according to Table (1), derived from the famous Scherrer equation [10]:

$$D = k' \lambda / \beta \cos\theta \qquad \text{.........} (1)$$

Within this range, k' might be anywhere from 0.89 to 1.39, with 0.9 often being the closest figure. This is the reason behind selecting an X-ray wavelength of 0.9 λ, where β represents the full-width at half of the most intense peak's maximum. (i.e. (110)) in radians, and θ is Bragg's angle for the purpose of calculating grain size. The calculated crystallite size values are also shown in Table (1). The film's average crystallite size is 24.6 nm when deposited, but it grows to 28.3 nm at annealing temperatures up to 400°C, but then decrease to 25.5 nm at 500°C. In other words, the maximum crystallinity occurs in the film annealed at 400 °C, the size of the crystallites in thin films is determined by the defect (fewer defects), where a low defect level indicates a high degree of crystallinity.

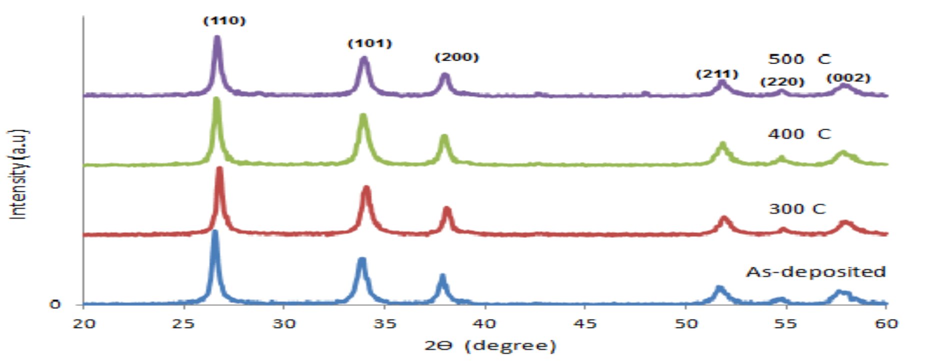

Fig. 2. XRD spectra of SnO2 films

Table (1) Interplanar distance between different planes and crystalline sizes for the SnO_2 thin films

Samples	Standard values		As-deposited at 200°C		Annealed at 300°C		Annealed at 400°C		Annealed at 500°C	
(hkl)	2θ	d(Å)	2θ	d(Å)	2θ	d(Å)	2θ	d(Å)	2θ	d(Å)
(110)	26.61	3.351	26.58	3.350	26.81	3.323	26.67	3.339	26.69	3.336
crystalline sizes D nm			24.6		26.3		28.3		25.5	

The reflectance $R(\lambda)$ and transmittance $T(\lambda)$ spectra of SnO_2 films as-deposited and after they are annealed at 300, 400, and 500 °C with regard to wavelengths ranging from 300 to 900 nm are displayed in Figure (3) and Figure (4), respectively. Annealing films at higher temperatures results in more visible changes to the films' characteristics, such as an increase in transmittance and a reduction in reflectance. This is particularly true for films annealed between 300 and 400°C.

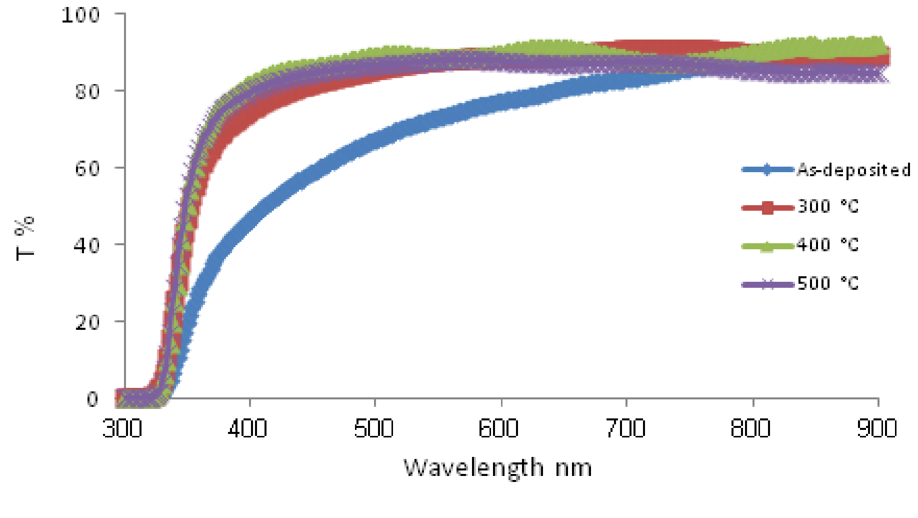

Fig(3) Transmittance spectra for the SnO2 thin films

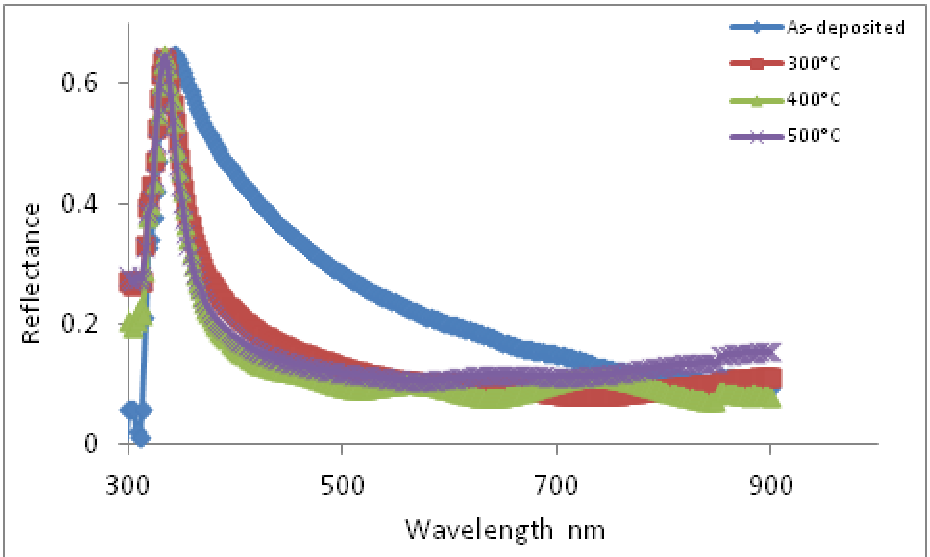

Fig (4) reflectance spectra of SnO_2 thin films

Using the measured values of transmission (T) The following equation was used to get the absorption coefficient α [5]:

$$\alpha = \frac{1}{t}\ln(1/T) \qquad \text{..........(2)}$$

Where t is the films thickness.

Using the following formula, the direct optical band gap Eg was calculated [5]: $\alpha h\upsilon = \beta_o \left(h\upsilon - E_g\right)^{\frac{1}{2}}$ .... (3)

To determine the optical band gap of thin films, the relationship between photon energy (hυ) and the square of the thickness (αhυ) was plotted, as seen in Figure 5, and the intercept of the curve with the hυ axis was calculated, where βo is a constant. Band gap energies are expected and may be found in Table 2. The Eg of the films is 3.68 eV when deposited, 3.72 eV after annealing at 400 ℃, and 3.7 eV after cooling to 500 ℃. An expansion of the optical band gap When the annealing temperature is raised, unsaturated defects are gradually removed, increasing the number of saturated bonds. As a result, the optical gap widens and the density of localized states decreases [11]. However, as demonstrated by XRD, the energy gap decreases as annealing is raised to 500 ℃, leading to a rise in defects and a decrease in crystallinity. The Eg values obtained by Camacho et al. are comparable to these [6]. While H. A. Mohamedand, N. M. A. Hadia at 500 °C, an impressive 3.65 eV optical energy-gap was attained [8]. The band gap of the orthorhombic SnO_2 phase is reportedly greater than that of the tetragonal phase, according to certain studies. The band gap of orthorhombic SnO_2 that has been laser ablated was found to be 3.79 eV by Kong et al. [12]. Orthorhombic SnO_2 thin films produced by laser ablation were reported by Chen to have a value of 4.02 eV [13]. The band gap at 300 K for bulk tetragonal SnO_2 is 3.6 eV [14].

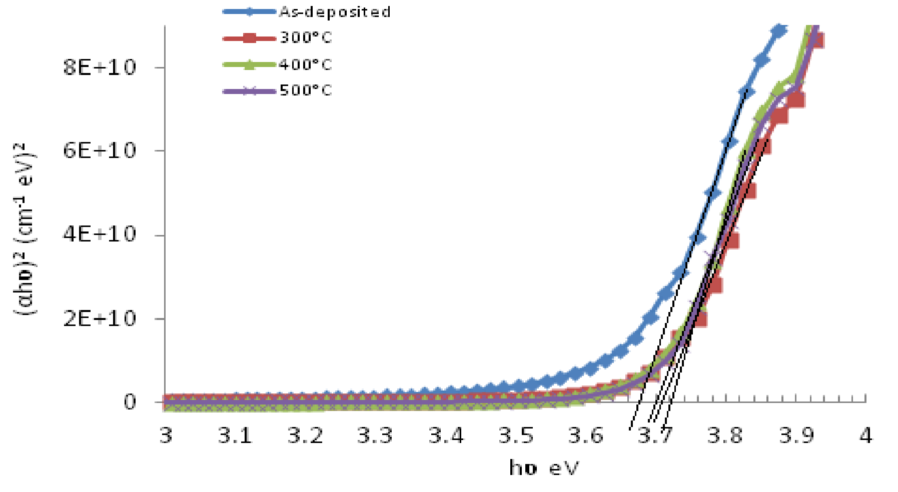

Fig(5) plote $(\alpha h\upsilon)^2$ versus hυ for SnO_2 thin films

Optical parameters namely, refractive index n and extinction coefficient k, dielectric constant real part ε_r and imaginary part ε_i have been determined by using the flowing relations [8,11,15,16]

$$k = \frac{\alpha\lambda}{4\pi} \qquad \text{............(4)}$$

$$n = \left[\left(\frac{1+R}{1-R}\right)^2 - \left(k^2+1\right)\right]^{\frac{1}{2}} + \frac{1+R}{1-R} \qquad \text{............(5)}$$

$$\varepsilon_r = n^2 - k^2 = \varepsilon_\infty - \left[\frac{e^2 N}{4\pi^2 c^2 \varepsilon_o m^*}\right]\lambda^2 \qquad \text{............(6)}$$

$$\varepsilon_i = 2nk = \left[\frac{\varepsilon_\infty \omega_p^2}{8\pi^2 c^3 \tau}\right]\lambda^3 \qquad \text{............(7)}$$

Where R is reflectance, e is the electronic charge and $\varepsilon_\infty$is the lattice dielectric constant, often known as the high frequency dielectric constant, ε_oIt can be noticed that the dependence of ε_r on λ^2 is linear at longer wavelengths, from the slope of liner part the ratios N/m* are computed and shown in Table (2). It is apparent that as the temperature at which annealing occurs increased up to 400℃, the values of the lattice dielectric constant ε_∞ and ratios N/m* fall. After that, they slightly rise, which may be connected to the variations of the energy gap.

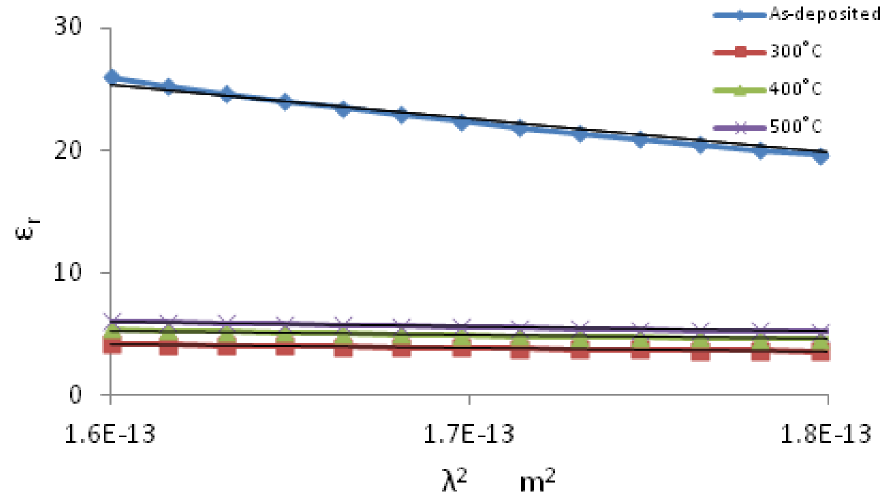

Fig(7) plots real part of dielectric constant versus λ^2 for SnO_2 thin films

Equation (7) is utilized to compute the imaginary component of the dielectric constant, which is then shown as a function of λ^2 in Figure (7). From the slope of liner part, the values of ω_p and τ are calculated. Where ω_p is equal to [15]:

$$\omega_p = \left[\frac{e^2 \; N}{\varepsilon_0 \; \varepsilon_\infty \; m^*}\right]^{\frac{1}{2}} \qquad \text{.............(8)}$$

The obtained ω_p and τ values are listed in Table (2). It is clear that the variation of optical relaxation time follows the same trend as the optical energy gap. Moreover, the plasma frequency decreases as the annealing temperature increases, which is directly correlated with the concentration of free carriers. [17].

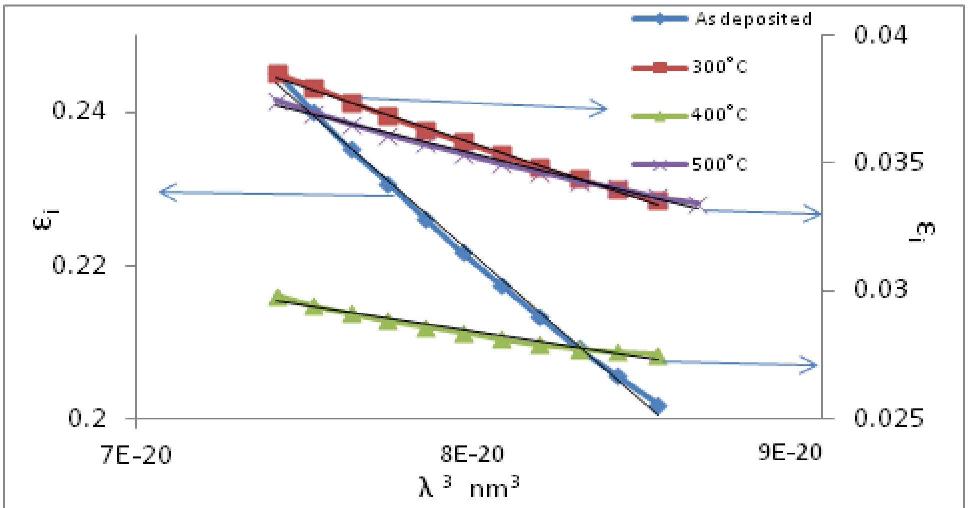

Fig(7) plots imaginary part of dielectric constant versus λ^3 for SnO_2 thin films

Table (2) Optical parameters for the thin films of SnO2 at different temperatures of annealing

Parameters / Samples	Eg eV	ε_∞	N/m* $x10^{58}$ m^{-3}	ω_p $x10^{15}$ s^{-1}	τ $x10^{-13}$ s
As deposited	3.68	68.87	65.00	5.2	2.2
Annealed at 300˚C	3.71	10.37	6.45	4.7	2.7
Annealed at 400˚C	3.72	8.32	6.40	4.2	4.4
Annealed at 500˚C	3.7	11.68	8.54	4.6	3.9

The dispersion behavior affects optical communication and the design of devices for spectrum dispersion, it is a crucial aspect of optical material research. Wemple–DiDomenico (W–D) dispersion model, a single-oscillator model of the following form, is used to analyze experimental refractive index data, which typically yields physically meaningful quantities like the oscillator energy and dispersion energy in transparent region for different solids [8,15]:

مجلة كلية التربية الاساسية
كلية التربية الاساسية – الجامعة المستنصرية
Journal of the College of Basic Education Vol.30 (NO. 125) 2024, pp. 1-16

$$n^2 - 1 = \frac{E_d\, E_o}{E_o^2 - (h\upsilon)^2} \qquad \text{......... (9)}$$

where the dispersion energy, or average intensity of the interband optical transitions, is expressed as E_d, and the oscillator energy with a single effective is expressed as E_o. The dispersion parameters (E_o and E_d) for every SnO_2 thin film are found by graphing $(n^2 - 1)^{-1}$ versus $(h\upsilon)^2$, as Figure (8) illustrates. Using the slope $(E_oE_d)^{-1}$ and the intercept on the vertical axis (E_o/E_d), and then can compute the principle of E_o and E_d.

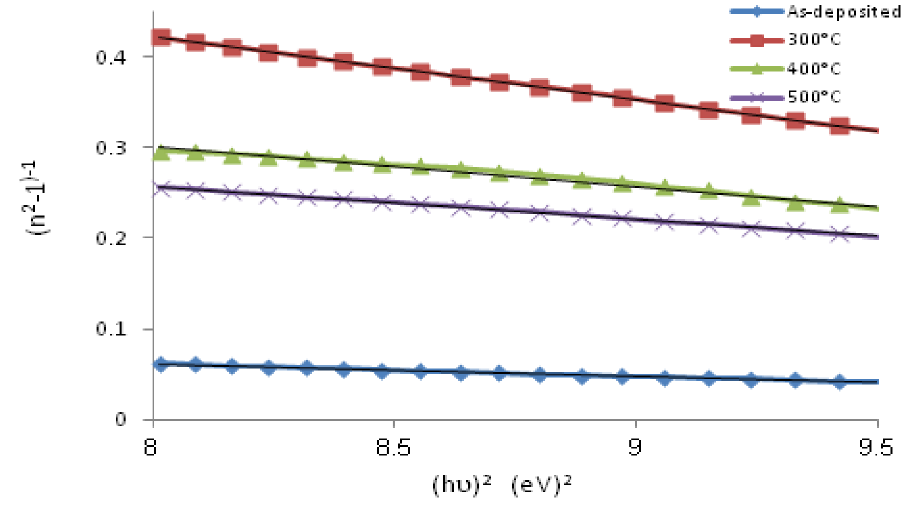

Fig(8) $(n^2-1)^{-1}$ versus $(h\upsilon)^2$ for SnO_2 thin films

Afterward, the following relationships can be used to derive the values of the optical spectrum's moments, $M_{-1}$and M_{-3} [8,18]:

$$E_o^2 = \frac{M_{-1}}{M_{-3}} \qquad \text{……….. (10)}$$

$$E_d^2 = \frac{M_{-1}^3}{M_{-3}} \qquad \text{………..(11)}$$

Table (3) lists the principles of E_d, E_o, M_{-1} and M_{-3}. The optical energy gap and dispersion energy Ed behave in the opposite way, whereas the principles of E_o, M_{-1} and M_{-3} fall at an annealed temperature of 400°C and begin to grow at high annealing temperatures.

Table (3) Optical dispersion parameters

Samples	Eg eV	E_o eV	E_d eV	M_{-1}	M_{-3} $(eV)^{-2}$	E_o/Eg
As deposited	3.68	4.35	15.56	4.35	0.23	1.18
Annealed at 300˚C	3.72	4.78	15.36	3.21	0.14	1.29
Annealed at 400˚C	3.71	4.92	14.61	2.96	0.12	1.33
Annealed at 500˚C	3.70	4.59	15.63	3.41	0.16	1.24

The Sellmeier dispersion formula [19] may also be used to examine the refractive index dispersion data, and it is provided by:

$$n^2 - 1 = \frac{\lambda_o^2 \; S_o}{1-\left(\frac{\lambda_o}{\lambda}\right)^2} \qquad \text{.............. (12)}$$

Where λ_o is the average oscillator wavelength, S_o is the oscillator strength. Figure 9 illustrates the relationship between $(n2\ -1)^{-1}$ and λ^2 for the SnO_2 films. From the slope $(1/S_o)$ and intercept $(1/S_o\lambda_o^2)$, which are stated in Table (4), we may estimate the values of S_o and λ_o. Table (4) displays the relationship between the annealing temperature and the average oscillator wavelength of SnO_2. In contrast to λ_o, which exhibits the opposite pattern, S_o values drop during annealing and reach a low of $0.51x10^{13}$ at an annealed temperature of 400°C. They slightly rise at higher temperatures, which might be explained by variations in the optical energy gap.

مجلة كلية التربية الاساسية
كلية التربية الاساسية – الجامعة المستنصرية
Journal of the College of Basic Education Vol.30 (NO. 125) 2024, pp. 1-16

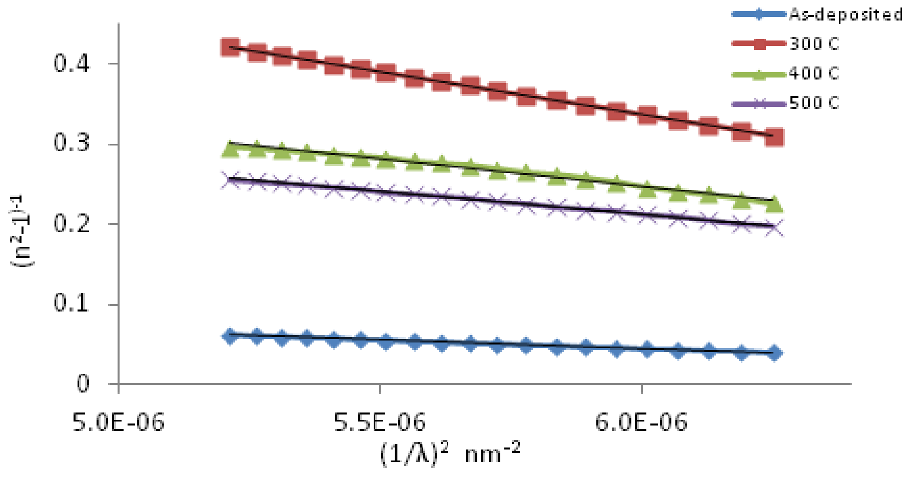

Fig (9) $(n^2-1)^{-1}$ versus $1/\lambda^2$ for SnO_2 thin films

There has been a rise in interest in using transparent heat mirror coatings, which are made of transparent conducting oxides and have a low thermal emissivity, to reduce heat radiation loss through window panes. This is motivated by concerns about the environment and sustainability [20]. The following relation can be used to determine the thermal emissivity $\in$ [21]:

$$\in = 1 - (T_{IR} + R_{IR}) \qquad \text{..........(13)}$$

The relationship between the temperature during annealing and the thermal emissivity of SnO_2 films is shown in Table (4), where T_{IR} and R_{IR} in the near-infrared band (λ=900 nm) are the average transmittance and reflection, respectively. Obviously, the variance of thermal emissivity maintains a similar pattern to the average oscillator wavelength as shown in Table (3).

The optical resistivity ρ_{opt} of SnO_2 films are determined by applying the subsequent formula [22]:

$$R = 1 - 4(\varepsilon_o c / t)\rho_{opt} \qquad \text{...........(14)}$$

Wherever, t is film thickness. As seen from the Table (4) shows the optical resistivity of SnO_2 values increase with annealing temperature increasing to 400 ^oC and then decreasing to 500 ^oC. This variation due to the change in the carrier concentration ratio to the effective mass is known as a free carrier concentrations.

Table (4) **oscillator strength, oscillator wavelength, optical resistivity and thermal emissivity of SnO_2 thin films**

Parameters / Samples	S_o m^2 X10^{13}	λ_o m x10^{-7}	$\rho_{optical}$ Ω.m X10^{-5}	ϵ X10^{-3}
As deposited	4.74	3.22	6.37	12.74
Annealed at 300˚C	1.47	3.51	6.84	0.39
Annealed at 400˚C	0.51	4.49	6.94	0.14
Annealed at 500˚C	1.77	3.20	6.72	0.44

Conclusion:

Thin films of SnO_2 deposited using the DC magnetron sputtering method on glass substrates and influence of annealing temperature on films' optical and structural characteristics was investigated. The thin-film XRD analysis indicated polycrystalline SnO_2 tetragonal structure with the best crystallinity obtained at 400˚C. The results showed that as the temperature during annealing increased to 400˚C, the following parameters decreased: high frequency dielectric constant, N/m*, plasma frequency, dispersion energy, specific optical spectrum moments, oscillator strength, and thermal emissivity. On the other hand, optical energy gap, optical relaxation time, oscillator energy, oscillator wavelength, and optical resistivity all showed mild increases. Based on the results shown above, it might be inferred that the SnO_2 thin films produced using the DC magnetron sputtering technique and annealed at 400˚C are of high quality. These films are ideal for use as transparent conducting oxides (TCOs) in various opto-electronic devices and can also be applied as heat mirror coatings.

Acknowledgments

Middle Technical University، which the authors would like to appreciate.

References

1- F. Liaqat, U. Vosqa, F. Khan, A. Haleem, M. Shaik, M. Rafiq, H. Siddiqui, and M. Khan " Light-Driven Catalytic Activity of Green-Synthesized SnO_2/WO3–x Hetero-nanostructures", CS Omega, 8 (22) (2023) 20042–20055.
2- S. Sagadevan, J. Podder," Nonlinear optical properties of cobalt doped SnO_2 thin films ", Optik, 272 (2023)170296.
3- M. Ghanaatshoar, M. Moradi, Z. Khodabandeh ," Magnetic and optical properties of fe-doped SnO_2 thin films prepared by electron beam evaporation technique", Journal of Superconductivity and Novel Magnetism, 26 (2013) 995–999.
4- G. Ramanathan, R. J. Xavier and K. R. Murali," Sol gel dip coated tin oxide thin films", Elixir Thin Film Technology, 50 (2012) 10588-10590.
5- S. S. Roy and J. Podder," Synthesis and optical characterization of pure and Cu doped SnO_2 thin film deposited by spray pyrolysis", Journal of Optoelectronics and Advanced Materials 12 (7)(2010) 1479-1484.
6- M. A.C.López, J. R.G.Camacho, A.E.García, C.S.Pérez, Julien C. M, "Characterization of nanostructured SnO_2 films deposited by reactive DC-magnetron sputtering", Superficies y 26 (3) (2013)95-99.
7- P.M. Gorley, V.V. Khomyak, S.V. Bilichuk, I.G. Orletsky, P.P. Horley, V.O. Yitian Ma, Ji Qian, W. Qu, R. Luo, F. Wu, R. Chen, "Materials and structure engineering by magnetron sputtering for advanced lithium batteries ", Energy Storage Materials, 39 (2021) 203-224.
8- H. A. Mohamedand N. M. A. Hadia, "Influence of post thermal annealing on the optical properties of SnO2 films Prepared by electron beam evaporation technique", International Journal of Thin Films Science and Technology, 4 (1) (2015) 1-7.
9- C.Coskun ¸ H.Guney, E.Gur and S.Tuzemen," Effective Annealing of ZnO Thin Films Grown by Electrochemical Deposition Technique", Turkish Journal of Physics , 33 (2009) 49-56.
10- Andrei A. Bunaciu, lena gabriela Udriştioiu, Hassan Y. Aboul-Enein ," X-Ray Diffraction: Instrumentation and Applications,", Critical Reviews in Analytical Chemistry , 45 (4) (2015).
11- P. Priyadarshini, D. Sahoo, R. Naik, "A review on the optical properties of some germanium based chalcogenide thin films and their applications", Optical and Quantum Electronics, 54 (166) (2022).
12- L.Kong, J.Ma, Z.Zhu, C.Luan, X.Yu, Q.Yu, " Synthesis of orthorhombic structure pitaxial tin oxide film", Materials Letters, 64, 30 (2010)1350-1353.
13- Z. W Chen., C. M. L.Wu, C. H.Shek, K. L.Lai J, Z.Jiao, M. H.Wu, "Pulsed Laser Ablation for Tin Dioxide: Nucleation, Growth, and Microstructures" , Critical Reviews in Solid State and Materials Sciences ,33 (3-4) (2008) 197-209.
14- K. K. Singha, P. P. Singh, R. Narzary, A. Mondal, M. Gupta, V. G. Sathe, D. Kumar and S. K. Srivastava, " Crystal Structure, Raman Spectroscopy and Optical Property Study of Mg-Doped SnO2 Compounds for Optoelectronic Devices ", Crystals 13(6) (2023) 932.
15- A. Bakry, " Dispersion and Fundamental Absorption Edge Analysis of Doped a-Si:H thin Films I : p-type", Egypt, Journal. Solids, 31 (2) (2008) 191-204.
16- T.S.Moss, G.J. Burrell, E. Ellis, Semiconductor Opto- Electronics, Butterworths, London ,1973.
17- A. Koch, H. Mei, J. Rensberg, M. Hafermann, J. Salman, Ch. Wan, R. Wambold, D. Blaschke, H. Schmidt, ü. Salfeld, S. Geburt, M. A. Kats, and C. Ronning," Heavily Doped Zinc Oxide with

Plasma Frequencies in the Telecommunication Wavelength Range ", dvanced Photonics Research published by Wiley-VCH GmbH, 4 (2023) 2200181-2200188.

18- F. Yakuphanoglu, S. Ilican, M. Caglar, Y. Caglar, "Synthesis, characterization, and nonlinear optical properties of copper (II) ligand Schiff based complexes derived from 3-nitrobenzohydrazide and benzyl", Scientific Reports, 13 (10988) (2023).

19- V. Gowthami, M.Meenakshi, P. Perumal, R. Sivakumar, C. Sanjeeviraja," Optical dispersion characterization of NiO thin films prepared by nebulized spray technique", International Journal of Chem Tech Research, 6(13) (2014) 5196-5202.

20- Z. Z. You and G. J. Hua, " Global technological advancement and challenges of glazed window, facade system and vertical greenery-based energy savings in buildings: A comprehensive review ", Energy and Built Environment, 4 (2) (2023) 206-226.

21- A. Metallo, " Emissivity Prediction for an IR Camera During Laser Welding of Aluminum ", nternational Journal of Thermodynamics (IJoT), 25 (4) (2022) 24-34.

22- C. H. L. Weijtens and P. A. C. Van loon, " Influence of Post Thermal Annealing on the Optical Properties of SnO_2 Films Prepared by Electron Beam Evaporation Technique. International Journal of Thin Films Science and Technology, 4 (1) (2015) 1-7.

مجلة كلية التربية الاساسية
كلية التربية الاساسية – الجامعة المستنصرية
Journal of the College of Basic Education Vol.30 (NO. 125) 2024, pp. 1-16

تأثير درجة حرارة التلدين على الخواص التركيبية والبصرية للأغشية الرقيقة SnO_2

هبه راشد شاكر
الجامعة التقنية الوسطى، معهد الطبي التقني – المنصور
hiba.rashid@mtu.edu.iq
07813427363
صلاح قدوري هزاع
جامعة الكرخ للعلوم، كلية العلوم، قسم الفيزياء الطبية، قسم تقنيات الفحص البصر
salah.hazaa@kus.du.iq
07703971667

مستخلص البحث:
تم تحضير الأغشية الرقيقة لأكسيد القصدير SnO_2 بواسطة تقنية الرش DC على ركائز زجاجية عند درجة حرارة 200 درجة مئوية. تم تلدين الأغشية المحضرة في الهواء عند درجات حرارة 300 و 400 و 500 درجة مئوية لمدة ساعة واحدة. تم دراسة تأثير درجة حرارة التلدين على الخواص التركيبية والبصرية للأغشية باستخدام مقياس حيود الأشعة السينية ومقياس الطيف الضوئي UV/VIS. أشارت أنماط حيود الأشعة السينية إلى أن الأغشية كانت أحادية الطور SnO_2 مع بنية رباعية البلورات. تمت دراسة الخصائص البصرية ومعايير التشتت للأغشية على طول موجي (300-900) نانومتر. تم تحقيق فجوة طاقة بصرية عالية تبلغ 3.72 الكترون فولت عند درجة حرارة 400 درجة مئوية. تم دراسة العديد من المعلمات الضوئية مثل معامل الانكسار، ثابت العزل الكهربائي، نسبة تركيز الموجة الحاملة إلى الكتلة الفعالة، طاقة المذبذب المفرد، طاقة التشتت، لحظات الطيف البصري، متوسط قيم قوة المذبذب، الطول الموجي للمذبذب المفرد، الموصلية الضوئية، الانبعاث الحراري وتم حساب وتحليل المقاومة الضوئية كدالة لدرجة حرارة التلدين.

الكلمات المفتاحية :
SnO_2، الخصائص البصرية، معاملات التشتت، التيار المستمر. تقنية الرشDC ، التلدين، الخصائص التركيبية.